ACS Catalysis

Research Article

Cite This: ACS Catal. 2019, 9, 8165−8170

pubs.acs.org/acscatalysis

Facile Protocol for Alkaline Electrolyte Purification and Its Influence on a Ni−Co Oxide Catalyst for the Oxygen Evolution Reaction

Ioannis Spanos,*[,†] Marc F. Tesch,[†] Mingquan Yu,[‡] Harun Tüysüz,[‡] Jian Zhang,[§] Xinliang Feng,[§] Klaus Müllen,[⊥] Robert Schlögl,[†,∥] and Anna K. Mechler*[,†]

[†]Department of Heterogeneous Reactions, Max Planck Institute for Chemical Energy Conversion, Stiftstrasse 34-36, 45470 Mülheim an der Ruhr, Germany

[‡]Department of Heterogeneous Catalysis and Sustainable Energy, Max-Planck-Institut für Kohlenforschung, Kaiser Wilhelm-Platz 1, 45470 Mülheim an der Ruhr, Germany

[§]Department of Chemistry and Food Chemistry, Center for Advancing Electronics, Zellescher Weg 19, 01069 Dresden, Germany

[∥]Department of Inorganic Chemistry, Fritz-Haber Institute of the Max Planck Society, Faradayweg 4-6, 14195 Berlin, Germany

[⊥]Department of Synthetic Chemistry, Max Planck Institute for Polymer Research Ackermannweg 10, 55128 Mainz, Germany

Supporting Information

ABSTRACT: We report a simple and effective electrochemical method to remove Fe impurities from commercial KOH electrolyte. We therefore utilize a MoS_2 catalyst deposited on porous Ni foam as both the anode and cathode in a two-electrode electrolysis setup. After 12 h of constant galvanostatic electrolysis at 100 mA, the Fe impurities from the KOH electrolyte were successfully removed, as confirmed by means of inductively coupled plasma optical emission spectroscopy analysis. In the purified KOH, a Ni−Co_3O_4 composite oxide catalyst showed no Fe-induced activation. In contrast, we directly observed the uptake of Fe on the Ni−Co_3O_4 catalyst from the nontreated electrolyte during catalyst operation using a coupled spectroelectrochemical setup. Interestingly, we further identified an influence on the dissolution behavior of Ni and Co in the presence of Fe impurities. Whereas hitherto mainly the activation effect of Fe impurities has been discussed, we hereby show that they additionally suppress corrosion under reaction conditions. Using our fast and low-cost method for the purification of large amounts of electrolyte, catalyst materials can be widely studied without these additional effects induced by Fe impurities in commercial KOH.

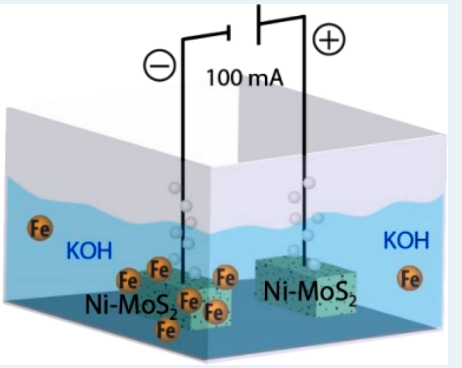

KEYWORDS: *oxygen evolution reaction, electrocatalysis, Fe impurities, KOH purification, ICP-OES*

The fraction of renewable energy has increased over the years to decrease the dependence on fossil-fuel-based energy resources like oil, coal, and so on. To store electrical energy from these more fluctuating sources, chemical energy conversion, for example, by water electrolysis, has been extensively investigated. New and efficient oxide catalyst materials based on Ir and Ru have been investigated under acidic and alkaline conditions.[1−6] However, the cost of such materials prohibits their use as catalysts for the oxygen evolution reaction (OER). Thus novel and cheap materials are necessary to replace the expensive and rare precious-metal-based catalysts. It is preferable that such materials should be based on abundant first-row transition metals like Fe, Ni, and Co.[7−14] Many studies have been focused on investigating Ni-based materials due to their excellent catalytic properties for the OER and on unraveling the mechanism behind the often-observed activity enhancement of Ni-based catalysts.[8,11,15−19] It is well established that $Ni(OH)_2$/NiOOH has a beneficial three-dimensionally porous brucite structure that facilitates easy ion transport and charge conductivity, which is ideal for water oxidation in alkaline. It has been proposed that the development of NiOOH species on the catalyst surface is responsible for the increased OER activity.[8,14−16] However, doping Ni-based catalysts with metals like Co, Mn, and Fe has shown enhanced catalytic activity due to changes in the electronic structure of the catalyst surface, with the Ni−Fe catalysts being the most active in the alkaline environment. It has also been pointed out that Fe impurities in the KOH electrolyte, which were formed during industrial production, might be a reason for the activation of Ni-based catalysts if they are incorporated into the catalyst structure.[14−16,20] The influence of Fe impurities, inherited in commercial KOH solution, on the activity and stability of Ni-based catalysts has drawn considerable attention. These previous studies have shown that Fe impurities, even on the order of ppm, can significantly alter the activity and stability of Ni-based catalysts,

Received: May 10, 2019
Revised: July 5, 2019
Published: August 1, 2019

especially for thin films. Considering the low Ni loading in the investigated films (i.e., 100 μg cm^{-2}), even Fe impurities in these low concentrations are expected to have a significant impact on the catalyst activity if they are incorporated into the Ni matrix. Also, to understand the role of Fe impurities in Ni-based catalysts, control measurements in an Fe-free KOH solution are critical. A well-established method by Trotochaud et al.[14] has been extensively used for the purification of KOH solution from unwanted Fe impurities. However, this method is complicated and costly considering the fact that it requires high-purity chemicals, that is, $Ni(NO_3)_2{\cdot}6H_2O$, and only small batches of electrolyte can be purified. On the contrary, here we present a method that can purify large batches of electrolyte, that is, 1 L or more, in a few hours.

In this work, we report an easy, cheap, and scalable electrochemical method for KOH electrolyte purification from unwanted Fe impurities with a MoS_2 catalyst deposited on a Ni foam forming NiS_3/MoS_2 heterostructures, from now on called Ni−MoS_2.[21] The above catalyst serves as both an excellent hydrogen evolution reaction (HER) and OER catalyst. Considering the fact that Ni-based catalysts become activated during water electrolysis due to Fe incorporation, we used Ni−MoS_2 as an active electrocatalyst with a high surface area to remove effectively all Fe impurities from the electrolyte. The advantage of this method is its applicability to large electrolyte volumes and the avoidance of additional chemical reagents.

The purification of 1 M KOH (in ultrapure water) was achieved in a two-electrode setup with the Ni−MoS_2 catalyst as both working electrode (WE) and counter electrode (CE) to actively remove Fe from the solution. Electrolysis at a constant current of 100 mA was conducted for 12 h while the solution was continuously circulated with a magnetic stirrer. Liquid samples were regularly extracted and analyzed by inductively coupled plasma optical emission spectroscopy (ICP-OES) to follow the Fe content in the electrolyte (Figure 1) and to exclude the possible addition of other contaminants

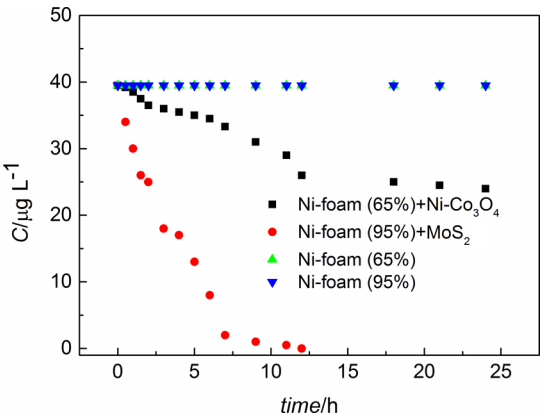

Figure 1. Fe content determination by means of ICP-OES on the 1 M KOH electrolyte at different intervals of the electrolysis purification procedure.

in the solution from the Ni foam electrodes, like Ni and Mo. As a comparison, the same purification methodology was used with three additional Ni-foam-based electrodes. Two Ni foams with different porosities (95 and 65%) used directly as the electrodes for the KOH purification were unsuccessful in removing Fe from the electrolyte, even after 25 h of constant electrolysis. In the case of the 65% porosity Ni foam, the same Ni−Co_3O_4 material, also investigated as an OER catalyst in this work, as described later, was deposited on the foam. Although this combined Ni foam/catalyst electrode was successful to a certain extent in removing almost half of the Fe content from the electrolyte, the stability issues of this electrode make it unsuitable for prolonged KOH purification.

On the contrary, with the MoS_2 catalyst on the high-porosity (95%) Ni foam after 12 h of electrochemical purification, the initial amount of ∼40 μg L^{-1} of Fe was completely removed from the electrolyte up to the detection limit of ICP-OES. No detectable amount of Fe or other metals was present in the electrolyte, and ∼1 L of KOH solution was effectively purified. Conveniently, in principle, this procedure can be straightforwardly scaled up by changing the size of the nickel foam and the electrolyte container.

To prove the presence of Fe on the catalyst, a Ni−MoS_2 foam used for five purifications of each 1 L of KOH solution was dissolved in aqua regia, followed by dilution in water at a ratio of 1/50. The amount of Fe on the Ni foam was measured with ICP-OES and was found to be ∼200 μg, which is the expected amount of Fe removed from 5 L of KOH electrolyte. The same procedure was conducted on the two pure Ni foams where no Fe removal was evident, and, as expected, no Fe could be detected.

Our results indicate the necessity of an additional active phase on a Ni foam to effectively remove Fe species from the electrolyte. However, in previous works, pure Ni foam was used to remove Fe impurities from a KOH electrolyte containing up to 1 ppm of Fe within 5 days of treatment.[22] The higher concentration of Fe and the long experimental time, which eventually leads to an activation of Ni by forming active surface species, might be the reason for the differences in the results. Nevertheless, we do not exclude that minor amounts of Fe can be removed by pure Ni foams even after a 24 h purification test, but those must be close to or below the detection limit of the ICP-OES. Therefore, if Fe removal indeed occurs on pure Ni, then it must be very slow under the given conditions. As a consequence, the formed Ni−MoS_2 phase can be identified as the active site for Fe removal. This is supported by the fact that NiS_3 materials show excellent HER and OER catalytic activity, with further catalytic gains when Fe is incorporated in the catalyst,[23−26] which is possibly also the case for Ni−MoS_2.

To elucidate this hypothesis, scanning electron microscopy (SEM) in combination with electron-dispersive X-ray spectroscopy (EDX) elemental mapping is shown in Figure 2.

Sulfur is located preferentially in the vicinity of molybdenum, supporting the presence of Ni−MoS_x species. Figure 2d furthermore shows a strong intensity of Fe signal close to Mo and S, indicating that Fe seems to preferentially deposit on these sites, although some signal can also be detected on the overall Ni foam. This observation supports the role of the Ni−MoS_2 species as active centers for the Fe removal from the electrolyte.

To test our purification method, we utilized the parallel analysis of catalyst corrosion and activity evaluation during an electrochemical benchmarking protocol on a Ni−Co_3O_4 composite catalyst. Our protocol is designed to test materials for their potential as efficient OER catalysts.[27]

The nanostructured nickel cobalt oxide catalyst used in this work has been prepared through a nanocasting approach using spent tea leaves as a sustainable template. (See Figure S1 for the catalyst characterization and description.)[11] A nickel to

DOI: 10.1021/acscatal.9b01940
ACS Catal. 2019, 9, 8165−8170

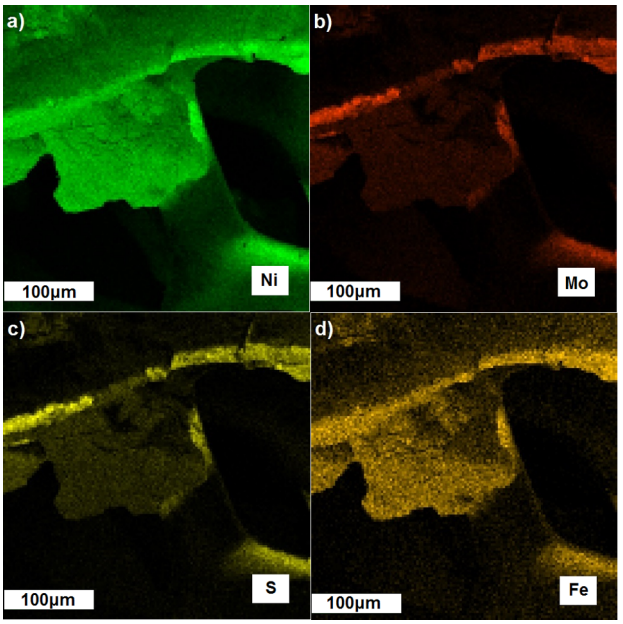

Figure 2. SEM/EDX-derived elemental mapping of a used Ni-MoS_2 catalyst with (a) Ni, (b) Mo, (c) S, and (d) Fe.

cobalt ratio of 1:4 was chosen, which has been reported to be the optimized composition for OER. Following a procedure detailed elsewhere,[28,29] conditioning of the Ni−Co_3O_4 composite was performed by applying 100 potential cycles between 0.7 and 1.6 V_{RHE} at a scan rate of 50 mV s^{-1}. Catalyst conditioning was followed by linear sweep voltammetry (LSV) to determine the activity of the catalyst, defined in this work as the maximum current density at 1.7 V_{RHE} after LSV between 1.2 and 1.7 V_{RHE} at a scan rate of 5 mV s^{-1}.

By combining electrochemical flow cell (EFC) measurements with online ICP-OES corrosion investigations, we were able to perform quantitative transient analysis of the catalyst corrosion products, like dissolved metal species of Co and Ni, and additionally for the first time, to the best of our knowledge, follow the Fe concentration of the KOH electrolyte during electrochemical testing. Thereby we can in situ investigate the Fe incorporation on the Ni−Co_3O_4 composite catalyst during a typical catalyst stress test. The Ni−Co_3O_4 catalyst corrosion behavior and Fe concentration in the electrolyte were investigated during a 2 h chronopotentiometric (CP) stress test at 10 mA cm^{-2}.

Figure 3 compares the stability, corrosion behavior, and Fe concentration changes in both Fe-contaminated and Fe-free KOH. Whereas with Fe in the electrolyte the potential initially drops, indicating catalyst activation, and thereafter remains stable over 2 h, it is initially higher in Fe-free KOH and continuously increases (Figure 3a). This already indicates a deactivation of the catalyst in the absence of Fe impurities, which is also reflected in the dissolution behavior (as explained later).

To prove the effect of Fe on the catalyst properties, the concentration of Fe in the electrolyte was monitored simultaneously along with the corrosion of Ni and Co during the 2 h stress test. The concentration of Fe found in the KOH electrolyte prior to the start of the stress test was 40 $\mu g\ L^{-1}$. With the start of the experiment, namely, applying a potential at t = 5 min (see the Experimental Section for details), an almost immediate drop of the Fe content of the KOH solution

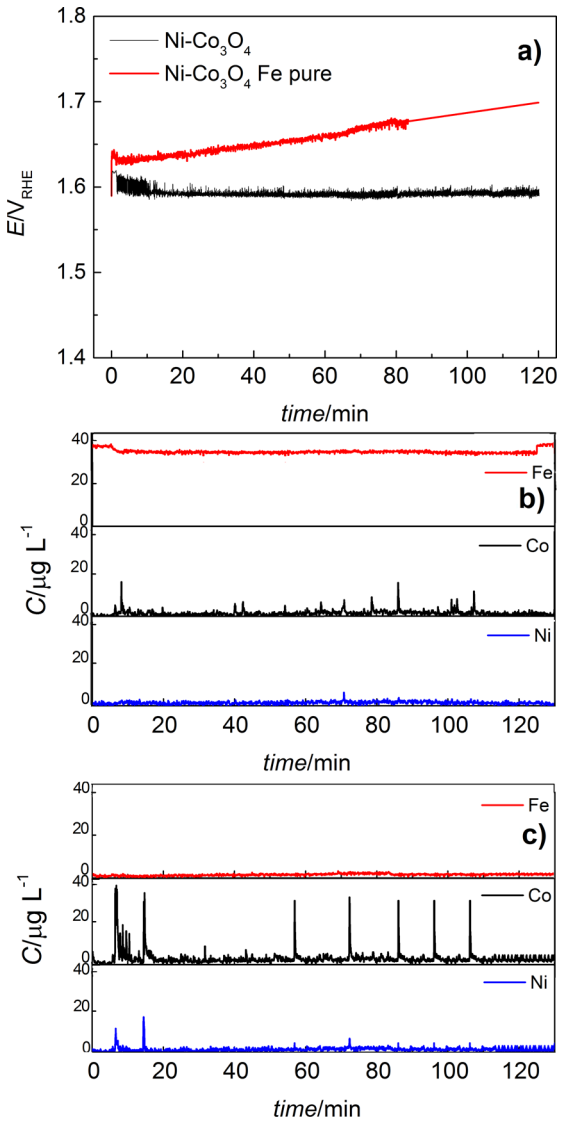

Figure 3. (a) Chronopotentiometry stress test profiles of the Ni−Co_3O_4 catalyst with and without Fe in solution at 10 mA cm^{-2} for 2 h. ICP-OES transient analysis of the corrosion products of the Ni−Co_3O_4 catalyst in (b) 1 M KOH Fe-contaminated and (c) Fe-free KOH solution. The Fe content of the KOH solution was monitored.

was observed (Figure 3b). The loss of Fe from the electrolyte suggests that a certain amount of Fe is incorporated on or into the catalyst surface. In contrast and as expected, in Fe-free KOH electrolyte, no Fe was detected in the solution (Figure 3c).

Interestingly, the dissolution of the Ni−Co_3O_4 sample in Fe-free electrolyte is also significantly affected. In the ICP-OES profiles, corrosion can be seen as signal spikes. Those spikes at different intervals of the ICP-OES profile signify material removal, which could, for example, be due to the accumulation of oxygen gas on the catalyst surface, accelerating material corrosion or catalyst detachment.

However, this gas accumulation must be small because the potential profiles of the catalyst in both electrolytes are smooth with no significant potential spikes (Figure 3a), which would otherwise indicate bubble formation on the catalyst surface. In the Fe-containing electrolyte, some small signals are visible for Co, indicating minimal Co corrosion, whereas Ni corrosion could not be detected (Figure 3b). However, in Fe-free KOH,

DOI: 10.1021/acscatal.9b01940
ACS Catal. 2019, 9, 8165−8170

significantly more intense spikes in the Co signal occur, and even Ni initially dissolves (Figure 3c). This shows that the incorporation of Fe on or into the Ni−Co_3O_4 catalyst not only changes the intrinsic activity but also critically influences the corrosion of Ni and Co from the catalyst. Even though in both electrolytes catalyst corrosion can be observed, in the case of Fe-free KOH, corrosion is significantly enhanced. This difference in corrosion rates probably affects the deactivation of the catalyst and explains the potential increase in Fe-free KOH.

As a comparison, the same experiment was conducted in 1 M KOH purified by the previously reported chemical method.[14] The Ni−Co_3O_4 catalyst showed exactly the same behavior regarding the activity, stability, and corrosion. (See Figures S2 and S3.) This confirms the good quality of the Fe-purified KOH produced by our simplified electrochemical method.

Besides the effect on the corrosion behavior during an electrochemical stress test, also the impact of the Fe impurities on the activity of the Ni−Co_3O_4 composite OER catalyst were investigated. Figure 4 shows the LSV curves of the Ni−Co_3O_4 composite before and after the 100 CV cycles of conditioning as well as after the 2 h stress test in both standard and Fe-free KOH. As expected, both curves of initial activity, before the 100 CV cycles, are only marginally different, which is expected due to the lack of any Fe incorporation on the Ni−Co_3O_4 catalyst. After the electrochemical treatment, the curves strongly deviate. In Fe-contaminated KOH, the catalyst is significantly activated after conditioning and even further activated after the 2 h CP stress test. In total, an almost two-fold activity increase can be observed, with a maximum current density increasing from 104 mA cm^{-2} at 1.7 V_{RHE} before the 100 CV cycles activation to 178 mA cm^{-2} after the chronopotentiometry stress test. In contrast, an overall activity drop is observed in the Fe-free KOH solution after both the conditioning and the 2 h stress test.

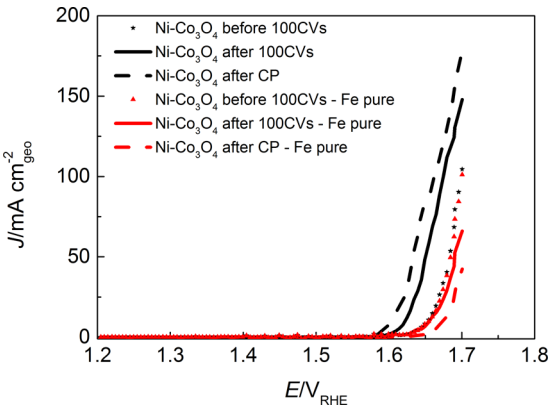

Figure 4. Activity comparison of the Ni−Co_3O_4 catalyst between 1.2 and 1.7 V_{RHE} at the 5 mV s^{-1} scan rate in Fe-contaminated (black) and Fe-pure (red) 1 M KOH.

Comparing the activity at 1.7 V_{RHE} of the Ni−Co_3O_4 catalyst after the 100 CV cycles conditioning between the Fe-contaminated and Fe-free KOH solutions, there is almost a 20% difference. This activity difference can be explained by some Fe incorporation already taking place during the conditioning step. After the 2 h stress test, this difference is further increased, indicating the severe influence of the Fe impurities on the catalytic activity of the Ni−Co_3O_4 catalyst during prolonged electrolysis.

Finally, to confirm the incorporation of Fe on the Ni−Co_3O_4 catalyst, the remaining catalyst was removed from the surface of the gold support after the 2 h stress test and was dissolved in concentrated HCl. After dilution, the acid solution was inserted into the ICP-OES for analysis. Because only part of the catalyst can be removed by this method, the amount of Fe detected on the remaining catalyst does not correspond to the total amount of Fe incorporated on the total 20 μg of catalyst initially deposited onto the support. To normalize the amount of Fe on the catalyst surface, the total detected amount of metals was scaled to fit the amounts of Ni and Co in 20 μg of pristine catalyst.

With this approach, the normalized Fe amount adsorbed into the catalyst was calculated to be ~0.5 μg. As a comparison, the incorporated Fe was calculated from the decrease in Fe concentration in the KOH solution during the 2 h stress test (Figure 3b), which was 0.52 μg. The similarity of the two methods confirms that the drop in concentration during the 2 h stress test can be assigned to an incorporation of Fe on the Ni−Co_3O_4 catalyst.

Considering the pristine atomic ratio of 4:1 for Co/Ni, calculated by ICP-OES measurements of a catalyst sample and the amount of incorporated Fe to be 0.52 μg, this corresponds to one Fe atom on every ten Ni atoms, which is reasonable considering the low amount of Fe contained in the electrolyte and, as a result, the even smaller amount incorporated.

To further prove the removal of Fe from KOH solution with our method, a second sample consisting of a mixture of NiO and CoO was tested.

The electrochemical and ICP-OES measurements showed similar behavior to that of the Ni−Co_3O_4 sample, that is, stable performance in Fe-containing KOH and deactivation in Fe-free KOH. For this second sample, additional soft X-ray absorption spectroscopy at the Fe L_3 edge in total electron yield mode was performed. For it, the catalyst was measured in its pristine form and after electrochemical measurements in Fe-containing and Fe-free KOH solution, respectively. Although these measurements do not allow the quantification of the incorporated Fe on the catalyst, they are very surface-sensitive and therefore ideal to detect even small amounts of Fe on the surface of the catalyst. Indeed, a clear Fe absorption feature reveals the presence of Fe for the sample that was treated in the Fe-containing KOH solution (Figure S4). Importantly, no Fe was detected in the pristine form of the catalyst and after electrochemical treatment in Fe-free KOH solution, further corroborating the quality of purification by our approach.

In this work, we have demonstrated a simple electrochemical purification technique with the use of a Ni−MoS_2 catalyst deposited on a Ni foam, thus making Fe-free KOH easily available for widespread applications. Whereas a pure Ni foam was ineffective for Fe removal, Ni−MoS_2 proved to be the active species that efficiently captures Fe from the electrolyte. In situ ICP-OES analysis could, for the first time, monitor the uptake of Fe from the solution during the electrochemical testing of a Ni−Co_3O_4 OER catalyst. Additionally, a significantly higher Ni and Co corrosion was detected in Fe-free KOH compared with the Fe-contaminated KOH, signifying the effect of Fe not only on activating the catalyst but also on preventing its degradation. This proves the high impact of even minimal impurities, as in this case of Fe, on the proper analysis of electrocatalysts for energy conversion and

DOI: 10.1021/acscatal.9b01940
ACS Catal. 2019, 9, 8165−8170

the necessity to review former and future publications with regard to the possible activation and stabilization of Ni-based catalysts during OER by Fe incorporation.

EXPERIMENTAL SECTION

The electrolyte purification was performed electrochemically in a two-electrode setup with a NiS_3−MoS_2 catalyst deposited on Ni foam electrodes of 3 × 1 cm^2 geometric surface area with a high porosity of 95% (Goodfellow). The molar content of the MoS_2 catalyst on the Ni foam was 8%.[21] During the electrolysis, a constant current of 100 mA was applied in a 1 L standard polystyrene bottle. For a period of 12 h, samples were collected and analyzed with ICP-OES to detect the residual Fe content. The voltage supplied by the potentiostat was ∼1.9 V, with a constant decrease over the 12 h of electrochemical purification, indicating an activation of the Ni foam catalyst and signaling the Fe removal from the KOH electrolyte and the incorporation on the Ni foam electrode. Finally, the electrolyte was filtered and stored for further use, whereas the Ni foam electrodes were thoroughly washed with deionized water and dried under a stream of argon for several minutes. We found that they can be reused several times for purification.

All electrochemical measurements on the Ni−Co_3O_4 catalyst were performed in 1 M KOH (Fluka Honeywell) with internal resistance (IR) correction. A coil-shaped platinized platinum wire (PT-5W, 125 μm diameter, 99.99%, Science Products), placed along the flow channel following the electrolyte flow, was used as the CE, whereas the reference electrode (RE) (Hg/HgO, CH Instruments, CHI152, reference potential +0.098 V vs NHE) was inserted perpendicular to the electrolyte outlet channel. All potentials are expressed versus the reversible hydrogen electrode (RHE) potential scale. To exclude Pt corrosion and redeposition on the WE during the electrochemical testing, which could affect data evaluation, the same experiment was performed with a glassy carbon CE (Figure S5), giving similar results. The potentiostat used for the electrochemical measurements was a Bio-Logic SP-150 apparatus, and the embedded EC-Lab software was used to electrochemically monitor the catalysts. Catalysts were dropcasted on gold support measuring a surface area of 0.196 cm^2, previously polished with fine 0.05 and 1.0 μm alumina powder and ultrasonicated for 15 min in Milli-Q water. Catalyst inks were prepared by mixing 49% H_2O, 49% ethanol, and 2% Nafion solution (5 wt %) and exposed to ultrasonication for 30 min. Subsequently, a certain amount of catalyst ink was dropcasted on the glassy carbon WE to achieve a loading of 100 μg cm^{-2}. The catalyst ink was dried on the gold support under an argon stream for 30 min; finally, the WE sample holder was inserted into the flow cell.

The resulting electrolyte stream was continuously fed into the ICP-OES (Spectroblue EOP, Ametek) by means of a peristaltic pump at a flow rate of 0.86 mL min^{-1} through a quartz nebulizer operating at a nebulizer gas flow rate of 0.85 L min^{-1} (Ar, purity 99,999%). All stability tests in this work were performed in CP mode by applying constant 10 mA cm^{-2} current density and all current density values were geometric surface area normalized.

For all electrochemical characterization, a flow rate of 0.86 mL min^{-1} was used, which provides a good balance between the oxygen gas removal from the catalyst surface and the sufficient detection of the catalyst corrosion products in the ICP-OES. Lower flow rates prohibit reproducible experimental conditions due to excessive oxygen bubble formation at high current densities. Transient signals of Ni, Co, and Fe were continuously recorded with an integration interval of 100 ms and two sweeps per reading, and detection limits were 0.12 ppb for Ni and Co and 0.08 ppb for Fe according to the manufacturer. For background correction on the ICP-OES data, a 5 min time window before and after the 2 h CP analysis, without any current passing through the cell, was used to certify that no signal drift was observed.

Before the measurement, manual calibration was performed using seven standard solutions (50, 10, 1, 0.5, 0.1, 0.05, and 0 ppm metal, prepared from Merck CertiPUR). The plasma power was set to 1400 W with a plasma gas flow rate of 15 L min^{-1}.

For the synthesis of tea-leaf-templated Ni−Co_3O_4, the tea leaves from ceylon pure tea (Goran Mevlana) were utilized as a hard template after a washing treatment with hot water until the washing water became colorless. After drying at 80 °C under air, 30 g of tea leaves was added to an aqueous solution (300 mL) containing 12 g of $Co(NO_3)_2{\cdot}6H_2O$ and 3 g of $Ni(NO_3)_2{\cdot}6H_2O$. The stirring was conducted at room temperature for 2 h. After drying at 70 °C overnight, the obtained mixture was calcined in air at 550 °C for 4 h with a ramping rate of 2 °C min^{-1}. Finally, the product was obtained after being washed with 0.1 M HCl solution and cleaned with deionized water. NiO/CoO was purchased from Sigma-Aldrich.

The chemical Fe purification of KOH solution (as reference) was performed according to the procedure reported by Boettcher's group.[14] In brief, 2 g of 99.999% $Ni(NO_3)_2{\cdot}6H_2O$ was dissolved in 4 mL of 18.2 MΩ·cm H_2O in an acid-cleaned polypropylene centrifuge tube, followed by the addition of 20 mL of 1 M KOH into the tube to precipitate high-purity $Ni(OH)_2$. Afterward, the mixture was shaken for 30 min and the supernatant was decanted after centrifugation. The green solid was then washed with 18.2 MΩ·cm H_2O and 1 M KOH by redispersing the solid, centrifuging, and decanting the supernatant. 40 mL of 1 M KOH solution was added to the tube for purification. In brief, the solid was dispersed in KOH solution by shaking for 30 min to purify the Fe from the KOH solution, followed by 3 h of rest. The purified KOH solution was decanted after centrifugation and transferred to an acid polypropylene bottle.

X-ray absorption spectroscopy was carried out at the U49-2 PGM-1 beamline utilizing the LiXEdrom endstation at Helmholtz-Zentrum Berlin.

ASSOCIATED CONTENT

Supporting Information

The Supporting Information is available free of charge on the ACS Publications website at DOI: 10.1021/acscatal.9b01940.

Material characterization by means of SEM, XRD, and BET; supplementary catalyst activity and corrosion behavior in Fe-free electrolyte purified by a different methodology; XAS spectra; and electrochemical characterizations with a GC counter electrode (PDF)

AUTHOR INFORMATION

Corresponding Authors

*E-mail: ioannis.spanos@cec.mpg.de (I.S.).
*E-mail: anna.mechler@cec.mpg.de (A.K.M.).

DOI: 10.1021/acscatal.9b01940
ACS Catal. 2019, 9, 8165−8170

ORCID
Ioannis Spanos: 0000-0001-5737-4992
Xinliang Feng: 0000-0003-3885-2703
Klaus Müllen: 0000-0001-6630-8786
Anna K. Mechler: 0000-0002-0491-514X

Notes
The authors declare no competing financial interest.

■ ACKNOWLEDGMENTS

This work was supported by the MAXNET Energy consortium of the Max Planck Society. We acknowledge IMPRS-RECHARGE. We acknowledge Dr. Xiaohui Deng for his help during the catalyst preparation.

■ REFERENCES

(1) Cherevko, S.; Zeradjanin, A. R.; Topalov, A. A.; Kulyk, N.; Katsounaros, I.; Mayrhofer, K. J. J. Dissolution of Noble Metals during Oxygen Evolution in Acidic Media. *ChemCatChem* **2014**, *6*, 2219−2223.
(2) Diaz-Morales, O.; Raaijman, S.; Kortlever, R.; Kooyman, P. J.; Wezendonk, T.; Gascon, J.; Fu, W. T.; Koper, M. T. M. Iridium-based double perovskites for efficient water oxidation in acid media. *Nat. Commun.* **2016**, *7*, 12363−12368.
(3) Klemm, S. O.; Karschin, A.; Schuppert, A. K.; Topalov, A. A.; Katsounaros, I.; Mayrhofer, K. J. J. Time and potential resolved dissolution analysis of rhodium using a microelectrochemical flow cell coupled to an ICP-MS. *J. Electroanal. Chem.* **2013**, *693*, 127.
(4) Schuppert, A. K.; Topalov, A. A.; Katsounaros, I.; Klemm, S. O.; Mayrhofer, K. J. J. A Scanning Flow Cell System for Fully Automated Screening of Electrocatalyst Materials. *J. Electrochem. Soc.* **2012**, *159*, F670−F675.
(5) Seitz, L. C.; Dickens, C. F.; Nishio, K.; Hikita, Y.; Montoya, J.; Doyle, A.; Kirk, C.; Vojvodic, A.; Hwang, H. Y.; Norskov, J. K.; Jaramillo, T. F. A highly active and stable $IrO_x/SrIrO_3$ catalyst for the oxygen evolution reaction. *Science* **2016**, *353*, 1011−1014.
(6) Strickler, A. L.; Jackson, A.; Jaramillo, T. F. Active and Stable Ir@Pt Core−Shell Catalysts for Electrochemical Oxygen Reduction. *ACS Energy Letters* **2017**, *2*, 244−249.
(7) Burke, M. S.; Enman, L. J.; Batchellor, A. S.; Zou, S.; Boettcher, S. Oxygen Evolution Reaction Electrocatalysis on Transition Metal Oxides and (Oxy)hydroxides: Activity Trends and Design Principles. *Chem. Mater.* **2015**, *27*, 7549−7558.
(8) Burke, M. S.; Kast, M. G.; Trotochaud, L.; Smith, A. M.; Boettcher, S. Cobalt-iron (oxy)hydroxide oxygen evolution electrocatalysts: the role of structure and composition on activity, stability, and mechanism. *J. Am. Chem. Soc.* **2015**, *137*, 3638−48.
(9) Chen, C.; Kang, Y.; Huo, Z.; Zhu, Z.; Huang, W.; Xin, H. L.; Snyder, J. D.; Li, D.; Herron, J. A.; Mavrikakis, M.; Chi, M.; More, K. L.; Li, Y.; Markovic, N. M.; Somorjai, G. A.; Yang, P.; Stamenkovic, V. R. Highly Crystalline Multimetallic Nanoframes with Three-Dimensional Electrocatalytic Surfaces. *Science* **2014**, *343*, 1339.
(10) Deng, X.; Tüysüz, H. Cobalt-Oxide-Based Materials as Water Oxidation Catalyst: Recent Progress and Challenges. *ACS Catal.* **2014**, *4*, 3701−3714.
(11) Deng, X. H.; Chan, C. K.; Tüysüz, H. Spent Tea Leaf Templating of Cobalt-Based Mixed Oxide Nanocrystals for Water Oxidation. *ACS Appl. Mater. Interfaces* **2016**, *8*, 32488−32495.
(12) Fan, X.; Peng, Z.; Ye, R.; Zhou, H.; Guo, X. M3C (M: Fe, Co, Ni) Nanocrystals Encased in Graphene Nanoribbons: An Active and Stable Bifunctional Electrocatalyst for Oxygen Reduction and Hydrogen Evolution Reactions. *ACS Nano* **2015**, *9*, 7407−7418.
(13) Grewe, T.; Deng, X.; Weidenthaler, C.; Schüth, F.; Tüysüz, H. Design of Ordered Mesoporous Composite Materials and Their Electrocatalytic Activities for Water Oxidation. *Chem. Mater.* **2013**, *25*, 4926−4935.
(14) Trotochaud, L.; Young, S. L.; Ranney, J. K.; Boettcher, S. Nickel-iron oxyhydroxide oxygen-evolution electrocatalysts: the role of intentional and incidental iron incorporation. *J. Am. Chem. Soc.* **2014**, *136*, 6744−53.
(15) Ahn, H. S.; Bard, A. J. Surface Interrogation Scanning Electrochemical Microscopy of Ni(1-x)Fe(x)OOH (0 < x < 0.27) Oxygen Evolving Catalyst: Kinetics of the "fast" Iron Sites. *J. Am. Chem. Soc.* **2016**, *138*, 313−8.
(16) Friebel, D.; Louie, M. W.; Bajdich, M.; Sanwald, K. E.; Cai, Y.; Wise, A. M.; Cheng, M.; Sokaras, D.; Weng, T.; Alonso-Mori, R.; Davis, R. C.; Bargar, J. R.; Norskov, J. K.; Nilsson, A.; Bell, A. T. *J. Am. Chem. Soc.* **2015**, *137*, 1305−13.
(17) Ma, T. Y.; Dai, S.; Jaroniec, M.; Qiao, S. Z. Metal-organic framework derived hybrid Co3O4-carbon porous nanowire arrays as reversible oxygen evolution electrodes. *J. Am. Chem. Soc.* **2014**, *136*, 13925−31.
(18) McCrory, C. C. L.; Jung, S.; Ferrer, I. M.; Chatman, S. M.; Peters, J. C.; Jaramillo, T. F. Benchmarking hydrogen evolving reaction and oxygen evolving reaction electrocatalysts for solar water splitting devices. *J. Am. Chem. Soc.* **2015**, *137*, 4347−57.
(19) Wang, J.; Cui, W.; Liu, Q.; Xing, Z.; Asiri, A. M.; Sun, X. Recent Progress in Cobalt-Based Heterogeneous Catalysts for Electrochemical Water Splitting. *Adv. Mater.* **2016**, *28*, 215−30.
(20) Klaus, S.; Cai, Y.; Louie, M. W.; Trotochaud, L.; Bell, A. T. Effects of Fe Electrolyte Impurities on Ni(OH)2/NiOOH Structure and Oxygen Evolution Activity. *J. Phys. Chem. C* **2015**, *119*, 7243−7254.
(21) Zhang, J.; Wang, T.; Pohl, D.; Rellinghaus, B.; Dong, R.; Liu, S.; Zhuang, X.; Feng, X. Interface Engineering of MoS_2/Ni_3S_2 Heterostructures for Highly Enhanced Electrochemical Overall-Water-Splitting Activity. *Angew. Chem.* **2016**, *128*, 6814−6819.
(22) Corrigan, D. A. The Catalysis of the Oxygen Evolution Reaction by Iron Impurities in Thin Film Nickel Oxide Electrodes. *J. Electrochem. Soc.* **1987**, *134*, 377−384.
(23) Cheng, N.; Liu, Q.; Asiri, A. M.; Xing, W.; Sun, X.; et al. A Fe-doped Ni3S2 particle film as a high-efficiency robust oxygen evolution electrode with very high current density. *J. Mater. Chem. A* **2015**, *3*, 23207−23212.
(24) Feng, L.-L.; Yu, G.; Wu, Y.; Li, G.-D.; Li, H.; Sun, Y.; Asefa, T.; Chen, W.; Zou, X. High-Index Faceted Ni3S2 Nanosheet Arrays as Highly Active and Ultrastable Electrocatalysts for Water Splitting. *J. Am. Chem. Soc.* **2015**, *137*, 14023−14026.
(25) Sitthikhankaew, R.; Predapitakkun, S.; Kiattikomol, R.; Pumhiran, S.; Assabumrungrat, S.; Laosiripojana, N. Comparative Study of Hydrogen Sulfide Adsorption by using Alkaline Impregnated Activated Carbons for Hot Fuel Gas Purification. *Energy Procedia* **2011**, *9*, 15−24.
(26) Zou, X.; Sun, Q.; Zhang, Y.; Li, G.-D.; Liu, Y.; Wu, Y.; Yang, L.; Zou, X. Ultrafast surface modification of Ni(3)S(2) nanosheet arrays with Ni-Mn bimetallic hydroxides for high-performance supercapacitors. *Sci. Rep.* **2018**, *8*, 4478−4478.
(27) Spanos, I.; Auer, A. A.; Neugebauer, S.; Deng, X.; Tüysüz, H.; Schlögl, R. Standardized Benchmarking of Water Splitting Catalysts in a Combined Electrochemical Flow Cell/Inductively Coupled Plasma−Optical Emission Spectrometry (ICP-OES) Setup. *ACS Catal.* **2017**, *7*, 3768−3778.
(28) Deng, X.; Chen, K.; Tüysüz, H. Protocol for the Nanocasting Method: Preparation of Ordered Mesoporous Metal Oxides. *Chem. Mater.* **2017**, *29*, 40−52.
(29) Deng, X.; Öztürk, S.; Weidenthaler, C.; Tüysüz, H. Iron-Induced Activation of Ordered Mesoporous Nickel Cobalt Oxide Electrocatalyst for the Oxygen Evolution Reaction. *ACS Appl. Mater. Interfaces* **2017**, *9*, 21225−21233.

DOI: 10.1021/acscatal.9b01940
ACS Catal. 2019, 9, 8165−8170